energy&fuels
ARTICLE
pubs.acs.org/EF

High-Pressure Biodiesel Density: Experimental Measurements, Correlation, and Cubic-Plus-Association Equation of State (CPA EoS) Modeling

Maria Jorge Pratas,[†] Mariana B. Oliveira,[*,†] Maria José Pastoriza-Gallego,[‡] António J. Queimada,[§] Manuel M. Piñeiro,[‡] and João A. P. Coutinho[*,†]

[†]Centre for Research in Ceramics and Composite Materials (CICECO), Department of Chemistry, University of Aveiro, Campus de Santiago, 3810-193 Aveiro, Portugal

[‡]Departamento de Física Aplicada, Facultade de Ciencias, Universidade de Vigo, E36310 Vigo, Spain

[§]Laboratory of Separation and Reaction Engineering (LSRE), Faculdade de Engenharia, Universidade do Porto, 4200-465 Porto, Portugal

S *Supporting Information*

ABSTRACT: Density is one of the most important biodiesel properties, because engine injection systems (pumps and injectors) must deliver an amount of fuel precisely adjusted to provide a proper combustion while minimizing greenhouse gas emissions. The pressure influence in fuel density has become particularly important with the increased use of modern common rail systems, where pressures can reach 250 MPa. Nevertheless, besides its importance, little attention has been given to high-pressure biodiesel densities. In fact, there are almost no reports in the literature about experimental high-pressure biodiesel density data. To overcome this lack of information, in this work, new experimental measurements, from 283 to 333 K and from atmospheric pressure to 45 MPa, were performed for methyl laurate, methyl myristate, and methyl oleate, for methyl biodiesels from palm, soybean, and rapeseed oils, and for three binary and one ternary mixture of these oils. Following previous works, where the cubic-plus-association equation of state (CPA EoS) was shown to be the most appropriate model to be applied to biodiesel production and purification processes, the new high-pressure experimental data reported here were also successfully predicted with the CPA EoS, with a maximum deviation of 2.5%. A discussion about the most appropriate CPA pure compound parameters for fatty acid methyl esters is also presented.

1. INTRODUCTION

Biodiesel has recently been the focus of increasing attention from researchers because of its rising use as a new energy solution to replace petroleum-based fuels. Its production has increased exponentially in the past decade, from worldwide negligible productions in 1990 to its production reaching over 2500 million tons in 2008. Biodiesel is the most used biofuel in Europe, reaching the 9.6 million tons of consumption.[1]

Besides its well-known environmental advantages over petroleum fuels,[2] biodiesel can be mixed in all proportions with regular diesel with no motor changes, is easier to store and transport, and has a more favorable combustion profile.[3,4] It consists of a blend of fatty acid esters that are industrially produced through the transesterification reaction of a vegetable oil or a fat with an alcohol, usually using a basic catalyst to increase the reaction speed and yield.[3] Rapeseed, soybean, and palm oils are the most commonly used oils to produce biodiesel.[5]

Nowadays, most new vehicles operate with common rail diesel engines, which use high injection pressures to allow for a rapid fuel atomization and combustion with consequent higher engine efficiencies and lower emissions.[6] Modern ultra-high-pressure injection systems can approach pressures of 250 MPa.[7]

Considering the predictable increase of biodiesel use, with Europe aiming to replace 20% of fossil fuels to alternative renewable fuels, such as biofuels, by 2020,[1] and the introduction of common rail engines in new vehicles, it is expected that these engines will work with biodiesel fuel blends with high biodiesel content and eventually even with pure biodiesels.

As Boudy and Seers[8] explained, from the evaluation of the effect of different fuel properties on the injection process of common rail direct-injection systems, density is the main property controlling the pressure wave in common rail systems and, subsequently, the total mass injected. NO_x emission increase from biodiesel use is partly related to the advancement of injection timing caused by the more rapid pressure wave transfer from the fuel injection pump to the fuel injector, causing it to open earlier.[9,10]

The European Committee for Standardization (CEN) has established quality standards specifying minimum requirements and test methods for biodiesels, the DIN EN 14214:2010,[11] including density specifications. However, these standards at ambient conditions can hardly be applied for common rail engines because densities suffer strong oscillations under high pressures.

Knowledge and description of biodiesel densities as a function of the pressure and temperature are therefore required for a correct biodiesel formulation and a proper design and optimization of

Received: June 1, 2011
Revised: July 25, 2011
Published: July 25, 2011

dx.doi.org/10.1021/ef200807m | *Energy Fuels* 2011, 25, 3806–3814

common rail engine injection systems for a precisely adjusted amount of fuel to be delivered to provide a proper combustion while minimizing NO_x emissions.[7] However, despite its importance, little attention has been given to high-pressure densities of biodiesels, and measurements and predictions of that property have been restricted to ambient conditions. Only Aparicio et al.[12,13] reported density measurements, in the temperature range from 288.15 to 328.15 K and pressure range from 0.1 to 350 MPa, for the rapeseed and sunflower oil methyl esters. Their experimental results were correlated with the modified Tait–Tammann equation.

After experimental data were reported for the atmospheric pressure temperature dependence of density for several fatty acid methyl and ethyl esters (from the most commonly found in biodiesel samples[14] to the less common[15]) for different biodiesels[16] and the best models were studied to predict the densities of biodiesel,[16] we carried out experimental high-pressure density measurements here for several of these pure compounds and biodiesels.

New high-pressure density data are reported in this work for three fatty acid methyl esters (FAMEs) and seven biodiesels, in the temperature range from 283 to 333 K and from atmospheric pressure to 45 MPa. Experimental densities were correlated using the modified Tait–Tammann equation,[17] and thermodynamic properties, such as isothermal compressibilities and isobaric expansion coefficients, were also calculated and evaluated, on the temperature and pressure ranges studied.

Empirical models, such as the modified Tait–Tammann equation, are the most commonly used to correlate high-pressure density experimental data. In this work, a different and completely predictive approach was also applied, which consisted of the use of the cubic-plus-association equation of state (CPA EoS) to describe the experimental data. In previous works,[18–20] the CPA EoS was shown to be the most appropriate model to be applied to biodiesel production and purification processes. A discussion about the most appropriate CPA pure compound parameters for esters is also presented.

2. EXPERIMENTAL SECTION

2.1. Materials. Experimental densities were measured for three pure methyl esters, methyl laurate and methyl myristate supplied by SAFC with purity of 98% and methyl oleate at 99% purity from Aldrich, and for seven different biodiesel samples. Biodiesels were synthesized by the transesterification reaction with methanol of the vegetable oils soybean (S), rapeseed (R), and palm (P) and their respective binary and ternary mixtures: soybean + rapeseed (SR), rapeseed + palm (RP), soybean + palm (SP), and soybean + rapeseed + palm (SRP). The molar ratio of oil/methanol used was 1:5 using 0.5% sodium hydroxide by weight of oil as a catalyst. The reaction was performed at 55 °C for 24 h under methanol reflux. The reaction time chosen was adopted for convenience and to guarantee a complete reaction conversion. Raw glycerol was removed in two steps: the first after 3 h of reaction and then after 24 h of reaction in a separating funnel. Biodiesel was purified through washing with hot distillated water until a neutral pH was achieved. The biodiesel was then dried until the EN ISO 14214 limit for water was reached (less than 500 mg/kg of water[11]).

Biodiesels were characterized by gas chromatography–flame ionization detector (GC–FID) following the British Standard EN 14103 from EN 14214[11] to know their methyl ester composition. Capillary GC was used to determine the methyl ester composition of the biodiesel samples. A Varian CP-3800 with a FID in a split injection system with a Select™ Biodiesel for FAME column (30 m × 0.32 mm × 0.25 μm) was used to differentiate all methyl esters in analysis, inclusive of the polyunsaturated ones. The column temperature was set at 120 °C and then programmed to increase to 250 °C at 4 °C/min. The detector and injector were set at 250 °C. The carrier gas was helium, with a flow rate of 2 mL/min.

2.2. Experimental Procedure. Experimental high-pressure densities were determined using an Anton Paar 512P vibrating tube densimeter, connected to an Anton Paar DMA 4500 data acquisition unit. This device determines the vibration period of a metallic U-shape cell filled with the studied fluid, which is directly linked to the sample fluid density. The calibration procedure used in this case has been described previously in detail[21,22] using water and vacuum as calibrating references. This method enables the highest accuracy in density determination over wide ranges of pressure, and even reliable density extrapolation can be performed. The repeatability in the density values determined from the vibration period measured by the DMA 4500 unit is 10^{-5} g cm^{-3}.

Temperature stability is ensured with a PolyScience 9510 circulating fluid bath, and the temperature value is determined with a CKT100 platinum probe placed in the immediacy of the density measuring cell, with an uncertainty that has been determined to be lower than 5×10^{-2} K.

The pressure is generated and controlled using a Ruska 7610 pressure controller, whose pressure stability is 2×10^{-3} MPa. The pumping hydraulic fluid (dioctylsebacate fluid) is in direct contact with the fluid sample inside the 1.59×10^{-3} m diameter steel pressure line conduction, with a coil designed to keep a distance (around 1 m) from the fluid contact interface to the measuring cell, avoiding any diffusion effect. The combinations of density determination repeatability and the accuracies in temperature and pressure measurement lead to an overall experimental density uncertainty value that is lower than 0.1 kg m^{-3} for the whole pressure and temperature range studied in this work.

3. DENSITY MODELS

3.1. Modified Tait–Tammann Equation. Liquid densities were correlated using the modified Tait–Tammann equation.[17] Other thermodynamic properties were also derived from this equation, such as the isothermal compressibility coefficient, k_T, and the isobaric expansion coefficient, α_P.

The following form of the modified Tait–Tammann equation[17] is used in this work:

$$\rho = \frac{\rho(T, P = 0.1\ \text{MPa})}{\left[1 - C \ln \dfrac{(B + P)}{(B + 0.1)}\right]} \tag{1}$$

where

$$\rho(T, P = 0.1\ \text{MPa}) = a_1 + a_2 T + a_3 T^2 \tag{2}$$

In eq 2, a_1, a_2, and a_3 are found by fitting to the experimental $\rho(T, P = 0.1\ \text{MPa})$.

Coefficient B is defined as

$$B = b_1 + b_2 T + b_3 T^2 \tag{3}$$

Coefficients C, b_1, b_2, and b_3 are also obtained by fitting the modified Tait–Tammann equation to the experimental data.

The Tait equation is an integrated form of an empirical equation representative of the isothermal compressibility coefficient behavior versus pressure. The effect of the pressure in density can be best described by the isothermal compressibility, k_T, which is calculated according to the following expression:

$$k_T = -\frac{1}{V_m}\left(\frac{\partial V_m}{\partial P}\right)_T = \frac{1}{\rho}\left(\frac{\partial \rho}{\partial P}\right)_T = \left(\frac{\partial \ln \rho}{\partial P}\right)_T \tag{4}$$

where ρ is the density and P is the pressure at a constant temperature, T. Isothermal compressibilities can be calculated using eqs 1 and 4.

$$k_T = \left(\frac{C}{B + P}\right)\left(\frac{\rho}{\rho(T, P = 0.1 \text{ MPa})}\right) \tag{5}$$

The isobaric expansion coefficient, α_P, is defined as

$$\alpha_P = \frac{1}{V_m}\left(\frac{\partial V_m}{\partial T}\right)_P = -\frac{1}{\rho}\left(\frac{\partial \rho}{\partial T}\right)_P = -\left(\frac{\partial \ln \rho}{\partial T}\right)_P \tag{6}$$

and the following expression is derived from the modified Tait−Tammann equation (eq 1)

$$\alpha_P = -\frac{[\mathrm{d}\rho(T, P = 0.1 \text{ MPa})/\mathrm{d}T]}{\rho(T, P = 0.1 \text{ MPa})} + C\left\{\frac{\frac{\mathrm{d}B}{\mathrm{d}T}(P - 0.1)}{\left[1 - C \ln\left(\frac{B + P}{B + 0.1}\right)\right](B + 0.1)(B + P)}\right\} \tag{7}$$

where $\mathrm{d}\rho(T,P = 0.1 \text{ MPa})/\mathrm{d}T = a_2 + 2a_3$ and $\mathrm{d}B/\mathrm{d}T = b_2 + 2b_3$.

3.2. CPA EoS. The CPA EoS[23−25] combines a physical contribution from a cubic EoS, in this work, Soave−Redlich−Kwong (SRK), with an association term accounting for intermolecular hydrogen bonding and solvation effects,[26,27] originally proposed by Wertheim and used in other association EoSs, such as the statistical associating fluid theory (SAFT).[28] The association term included in the CPA EoS allowed, in previous works from ours, for the correct description of the water solubility in fatty acid esters and biodiesels,[20] the atmospheric[29] and near/supercritical[30] vapor−liquid equilibria (VLE) of fatty acid ester + alcohol systems, and the liquid−liquid equilibria (LLE) of multicomponent systems containing fatty acid esters, alcohols, glycerol, and water,[18,19,31] because it can explicitly take into account the solvation phenomena found in these systems containing non-self-associating compounds (esters) that can associate with self-associating compounds, such as water, alcohols, and glycerol. Because, in this work, we are dealing with ester mixtures and because esters are known to not self-associate, the association term disappears from the CPA EoS and can be expressed in terms of the compressibility factor as

$$Z = \frac{1}{1 - b\rho} - \frac{a\rho}{RT(1 + b\rho)} \tag{8}$$

where a is the energy parameter, b the co-volume parameter, ρ is the molar density, and g is a simplified hard-sphere radial distribution function.

The pure component energy parameter, a, is obtained from a Soave-type temperature dependency.

$$a(T) = a_0[1 + c_1(1 - \sqrt{T_r})]^2 \tag{9}$$

Table 1. Compositions of the Biodiesels Studied, in Mass Percentage

methyl esters	S	R	P	SR	PR	SP	SRP
C10		0.01	0.03		0.02	0.01	0.01
C12		0.04	0.24	0.03	0.2	0.18	0.14
C14	0.07	0.07	0.57	0.09	0.54	0.01	0.38
C16	10.76	5.22	42.45	8.9	23.09	25.56	18.97
C16:1	0.07	0.2	0.13	0.15	0.17	0.11	0.14
C18	3.94	1.62	4.02	2.76	3.02	4.04	3.28
C18:1	22.96	62.11	41.92	41.82	52.92	33.13	42.51
C18:2	53.53	21.07	9.8	37.51	15.47	31.72	27.93
C18:3	7.02	6.95	0.09	7.02	3.08	3.58	4.66
C20	0.38	0.6	0.36	0.46	0.49	0.39	0.45
C20:1	0.23	1.35	0.15	0.68	0.67	0.2	0.52
C22	0.8	0.35	0.09	0.46	0.24	0.32	0.33
C22:1	0.24	0.19	0	0.12	0.09	0.12	0.14
C24		0.22	0.15			0.63	0.53

For mixtures, the energy and co-volume parameters are calculated, employing the conventional van der Waals one-fluid mixing rules

$$a = \sum_i \sum_j x_i x_j a_{ij} \quad a_{ij} = \sqrt{a_i a_j}(1 - k_{ij}) \tag{10}$$

and

$$b = \sum_i x_i b_i \tag{11}$$

As explained above, for non-associating components, such as esters, the association term disappears and CPA has only three pure component parameters in the cubic term (a_0, c_1, and b). These parameters are regressed simultaneously from vapor pressure and liquid density data. The objective function to be minimized is the following:

$$\mathrm{OF} = \sum_i^{N_p}\left(\frac{P_i^{\text{exptl}} - P_i^{\text{calcd}}}{P_i^{\text{exptl}}}\right)^2 + \sum_i^{N_p}\left(\frac{\rho_i^{\text{exptl}} - \rho_i^{\text{calcd}}}{\rho_i^{\text{exptl}}}\right)^2 \tag{12}$$

With this procedure, better density estimates are provided, overcoming SRK deficiencies in liquid-phase density estimates while leaving the possibility for future modeling in associating systems.

4. RESULTS AND DISCUSSION

Density measurements were carried out at temperatures ranging from 283.15 to 333.15 K and pressures from 0.10 to 45.0 MPa, for methyl laurate, methyl myristate, methyl oleate, rapeseed, soybean, and palm biodiesels, soybean + rapeseed biodiesel, rapeseed + palm biodiesel, soybean + palm biodiesel, and soybean + rapeseed + palm biodiesel.

Table 1 reports methyl ester compositions for the biodiesels selected for this work. This information is of major importance because the fatty acid ester profiles of biodiesels determine their chemical and physical properties, such as densities.[32] In addition, in a previous work of ours,[16] we showed the importance of knowing the detailed composition of biodiesels to compute their densities even with simple empirical models based on mixing rules and group contribution schemes. The experimental pressure−volume−temperature (PVT) data obtained are reported in Tables 2−4 for the pure FAMEs and biodiesels.

Table 2. Experimental Density Data for the FAMEs

	ρ (±0.1, kg m^{-3}) at T (±5 × 10^{-2}, K)					
p (±2 × 10^{-3}, MPa)	283.15	293.15	303.15	313.15	323.15	333.15
			Methyl Laurate			
0.10	877.1	869.3	861.4	853.5	845.8	837.6
1.00	877.7	869.9	862.0	854.2	846.5	838.4
2.00	878.4	870.6	862.7	854.9	847.2	839.2
3.00	879.1	871.2	863.4	855.7	848.0	840.0
4.00	879.7	871.8	864.0	856.3	848.7	840.7
5.00	880.3	872.5	864.7	857.1	849.5	841.5
10.0	883.3	875.6	867.9	860.4	853.0	845.3
15.0	886.2	878.5	871.1	863.7	856.4	848.7
20.0	889.0	881.5	874.2	866.9	859.8	852.2
25.0	891.6	884.3	877.1	870.0	863.0	855.8
30.0	894.3	887.1	879.9	872.9	866.1	859.0
35.0	896.9	889.7	882.7	875.9	869.1	862.1
40.0	899.3	892.4	885.4	878.7	872.0	865.1
45.0	901.7	894.9	888.1	881.4	874.8	868.0
			Methyl Myristate			
0.10		867.2	859.6	851.9	844.2	836.4
1.00		867.8	860.1	852.5	844.8	837.1
2.00		868.4	860.8	853.2	845.6	837.9
3.00		869.0	861.5	853.9	846.3	838.6
4.00		869.6	862.1	854.6	847.0	839.4
5.00		870.2	862.7	855.2	847.7	840.1
10.00		873.2	865.9	858.5	851.1	843.7
15.00		876.1	868.9	861.7	854.5	847.2
20.00		878.9	871.9	864.8	857.7	850.5
25.00		881.6	874.7	867.8	860.8	853.8
30.00		884.3	877.5	870.6	863.8	856.9
35.00		886.9	880.2	873.4	866.7	859.9
40.00		889.4	882.8	876.2	869.5	862.8
45.00		891.8	885.3	878.8	872.2	865.6
			Methyl Oleate			
0.10		873.8	866.6	859.3	852.0	844.8
1.00		874.4	867.2	859.9	852.7	845.5
2.00		875.0	867.8	860.6	853.4	846.2
3.00		875.6	868.4	861.2	854.1	846.9
4.00		876.2	869.0	861.9	854.7	847.6
5.00		876.7	869.6	862.5	855.5	848.3
10.0		879.7	872.6	865.6	858.7	851.7
15.0		882.4	875.5	868.7	861.8	855.0
20.0		885.0	878.3	871.6	864.9	858.3
25.0		887.7	881.1	874.4	867.9	861.3
30.0		890.2	883.7	877.2	870.7	864.4
35.0		892.7	886.2	879.8	873.6	867.2
40.0		895.1	888.8	882.5	876.3	869.9
45.0		897.5	891.2	885.0	878.8	872.7

Table 3. Experimental Density Data for the Methyl Biodiesels

	ρ (±0.1, kg m^{-3}) at T (±5 × 10^{-2}, K)					
p (±2 × 10^{-3}, MPa)	283.15	293.15	303.15	313.15	323.15	333.15
			R			
0.10	885.0	877.6	870.3	862.9	855.6	848.2
1.00	885.5	878.2	870.8	863.5	856.2	848.9
2.00	886.1	878.8	871.4	864.1	856.8	849.6
3.00	886.6	879.3	872.0	864.8	857.5	850.3
4.00	887.2	879.9	872.7	865.4	858.2	851.0
5.00	887.7	880.5	873.3	866.1	858.8	851.7
10.0	890.4	883.3	876.2	869.2	862.1	855.0
15.0	893.0	886.1	879.1	872.2	865.2	858.3
20.0	895.6	888.7	881.9	875.1	868.3	861.4
25.0	898.0	891.3	884.6	877.9	871.2	864.5
30.0	900.5	893.8	887.3	880.7	874.1	867.4
35.0	902.8	896.3	889.8	883.3	876.8	870.3
40.0	905.1	898.7	892.3	885.9	879.5	873.0
45.0	907.4	901.1	894.8	888.5	882.1	875.7
			P			
0.10	885.0	877.6	870.3	862.9	855.6	848.2
1.00	885.5	878.2	870.8	863.5	856.2	848.9
2.00	886.1	878.8	871.4	864.1	856.8	849.6
3.00	886.6	879.3	872.0	864.8	857.5	850.3
4.00	887.2	879.9	872.7	865.4	858.2	851.0
5.00	887.7	880.5	873.3	866.1	858.8	851.7
10.0	890.4	883.3	876.2	869.2	862.1	855.0
15.0	893.0	886.1	879.1	872.2	865.2	858.3
20.0	895.6	888.7	881.9	875.1	868.3	861.4
25.0	898.0	891.3	884.6	877.9	871.2	864.5
30.0	900.5	893.8	887.3	880.7	874.1	867.4
35.0	902.8	896.3	889.8	883.3	876.8	870.3
40.0	905.1	898.7	892.3	885.9	879.5	873.0
45.0	907.4	901.1	894.8	888.5	882.1	875.7
			S			
0.10	893.6	886.3	879.0	871.8	864.6	857.1
1.00	894.1	886.8	879.5	872.4	865.1	857.7
2.00	894.7	887.4	880.1	873.0	865.8	858.4
3.00	895.3	888.0	880.7	873.6	866.5	859.1
4.00	895.8	888.5	881.3	874.3	867.1	859.8
5.00	896.3	889.1	881.9	874.9	867.8	860.5
10.0	899.0	892.0	884.9	878.0	871.0	863.8
15.0	901.6	894.6	887.8	880.9	874.1	866.8
20.0	904.3	897.3	890.5	883.8	877.1	870.0
25.0	906.7	899.9	893.2	886.6	880.0	873.2
30.0	909.1	902.4	895.8	889.2	882.8	876.1
35.0	911.5	904.9	898.3	891.9	885.5	879.0
40.0	913.7	907.2	900.8	894.5	888.2	881.6
45.0	916.0	909.5	903.3	897.1	890.7	884.3

Considering high-pressure experimental measurements, only Aparicio et al.[12] reported previously data for the rapeseed methyl ester biodiesel. In the pressure range considered in this work, experimental rapeseed density values are in good agreement with the data reported by Aparicio and co-workers, as seen in Figure 1. It should be recalled, however, that no detailed biodiesel composition is reported by Aparicio et al.,[12] which limits the validity of a comparison because the compositions of the two fluids are not the same, as discussed elsewhere.[16] From the experimental results, it is possible to observe, for all of the pure compounds

Table 4. Experimental Density Data for the Methyl Biodiesels Obtained from Oil Binary and Ternary Mixtures

	ρ (±0.1, kg m^{-3}) at T (±5 × 10^{-2}, K)					
p (±2 × 10^{-3}, MPa)	283.15	293.15	303.15	313.15	323.15	333.15
SR						
0.10	891.2	883.9	876.7	869.4	862.5	854.9
1.00	891.7	884.5	877.2	870.0	863.0	855.5
2.00	892.3	885.1	877.8	870.7	863.7	856.2
3.00	892.8	885.6	878.4	871.3	864.3	856.9
4.00	893.4	886.2	879.0	872.0	865.0	857.6
5.00	893.9	886.8	879.6	872.6	865.6	858.3
10.0	896.6	889.6	882.6	875.7	868.8	861.7
15.0	899.3	892.3	885.5	878.6	871.9	864.7
20.0	901.8	894.9	888.2	881.5	875.0	867.9
25.0	904.3	897.6	890.9	884.3	877.9	871.1
30.0	906.7	900.1	893.5	887.0	880.8	874.0
35.0	909.2	902.5	896.1	889.7	883.4	876.8
40.0	911.3	904.9	898.6	892.3	886.2	879.5
45.0	913.6	907.3	901.0	894.8	888.7	882.3
RP						
0.10	886.3	879.0	871.7	864.3	857.0	849.7
1.00	886.8	879.5	872.2	864.9	857.6	850.3
2.00	887.4	880.1	872.8	865.6	858.3	851.1
3.00	888.0	880.7	873.4	866.2	859.0	851.8
4.00	888.5	881.3	874.1	866.8	859.6	852.4
5.00	889.1	881.9	874.7	867.5	860.3	853.1
10.0	891.8	884.7	877.6	870.6	863.5	856.5
15.0	894.5	887.5	880.5	873.6	866.7	859.8
20.0	897.1	890.2	883.3	876.5	869.7	862.9
25.0	899.6	892.8	886.0	879.3	872.6	866.0
30.0	902.1	895.4	888.7	882.0	875.4	868.9
35.0	904.5	897.8	891.2	884.7	878.2	871.8
40.0	906.9	900.3	893.7	887.3	880.9	874.6
45.0	909.1	902.6	896.2	889.8	883.5	877.3
SP						
0.10	887.4	880.1	872.8	865.5	858.2	850.8
1.00	887.9	880.6	873.3	866.1	858.8	851.5
2.00	888.5	881.2	874.0	866.7	859.5	852.2
3.00	889.0	881.8	874.6	867.3	860.1	852.9
4.00	889.6	882.4	875.2	868.0	860.8	853.6
5.00	890.1	882.9	875.8	868.6	861.5	854.3
10.0	892.8	885.8	878.8	871.7	864.7	857.7
15.0	895.5	888.5	881.6	874.8	867.9	861.0
20.0	898.0	891.2	884.4	877.7	870.9	864.1
25.0	900.5	893.8	887.2	880.5	873.8	867.2
30.0	902.9	896.4	889.8	883.2	876.7	870.1
35.0	905.3	898.8	892.4	885.9	879.5	873.0
40.0	907.6	901.2	894.9	888.5	882.1	875.8
45.0	909.9	903.6	897.3	891.0	884.8	878.5
SRP						
0.10	888.4	881.1	873.7	866.4	859.2	851.6
1.00	888.9	881.6	874.3	867.0	859.8	852.3
2.00	889.5	882.2	874.9	867.6	860.4	853.0
3.00	890.1	882.8	875.4	868.3	861.1	853.7
4.00	890.6	883.3	876.0	868.9	861.7	854.4
5.00	891.2	883.9	876.7	869.6	862.5	855.1
10.0	893.9	887.8	879.6	872.6	865.7	858.5
15.0	896.6	889.5	882.6	875.6	868.8	861.6
20.0	899.2	892.2	885.3	878.5	871.9	864.8
25.0	901.6	894.9	888.0	881.3	874.8	868.1
30.0	903.9	897.3	890.7	884.1	877.7	870.9
35.0	906.4	899.8	893.1	886.8	880.4	873.7
40.0	908.7	902.2	895.7	889.3	883.0	876.5
45.0	911.0	904.5	898.1	891.8	885.6	879.2

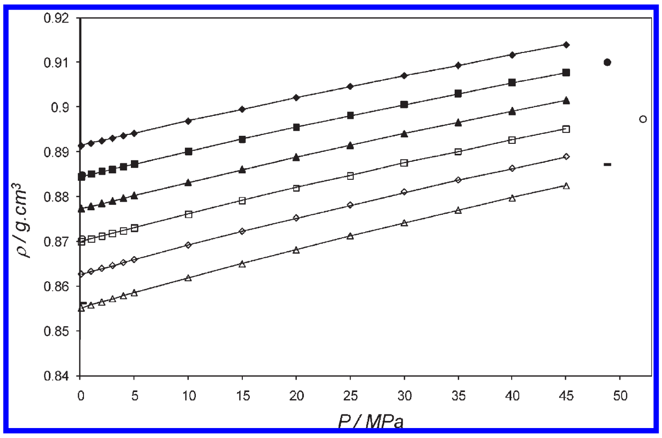

Figure 1. Density isotherms for rapeseed biodiesel. Experimental data from this work (◆, 283.15 K; ■, 293.15 K; ▲, 303.15 K; □, 313.15 K; ◇, 323.15 K; △, 333.15 K) and from the work by Aparicio et al.[12] (●, 288 K; ○, 308 K; -, 328 K) and modified Tait–Tammann equation results (solid lines).

Table 5. Equation 2 Coefficients

	a_1 (kg m^{-3})	a_2 (kg m^{-3} K^{-1})	a_3 (×10^7, kg m^{-3} K^{-2})
methyl laurate	1085.250	−0.69015	−1.5872
methyl myristate	1076.212	−0.66388	−1.6758
ethyl oleate	1092.999	−0.76617	0.6345
biodiesel R	1041.175	−0.36141	−5.9128
biodiesel P	1099.823	−0.77774	0.6757
biodiesel S	1085.338	−0.63419	−1.5251
biodiesel SR	1089.542	−0.68230	−0.6505
biodiesel RP	1095.181	−0.74229	0.1636
biodiesel SP	1093.702	−0.72685	−0.0637
biodiesel SRP	1088.614	−0.68473	−0.7922

and mixtures studied, that density decreases when both temperature increases and pressure drops. As expected, because a similar behavior was previously observed for pure unsaturated fatty acid esters,[14] biodiesel densities also increase with an increasing content of unsaturated FAMEs and their unsaturation level.

The modified Tait–Tammann equation was applied to correlate the experimental data. Coefficients a_1, a_2, and a_3 of eq 2 are presented in Table 5, and coefficients C, b_1, b_2, and b_3 for eq 3 are

Table 6. Coefficients of Equations 1 and 3, along with Average Absolute Deviation (AAD) from the Modified Tait−Tammann Equation

	C	b_1	b_2 (MPa)	b_3 ($\times 10^{-4}$, MPa K)	AAD (%)
methyl laurate	0.08803	466.39	−1.6886	16.9517	0.008
methyl myristate	0.08715	580.56	−2.3911	28.0143	0.006
methyl oleate	0.08486	510.32	−1.9231	20.5896	0.003
biodiesel R	0.08698	414.00	−1.2517	9.7351	0.006
biodiesel P	0.08776	683.20	−2.9750	37.1266	0.009
biodiesel S	0.08787	520.22	−1.9201	20.3902	0.007
biodiesel SR	0.08973	595.81	−2.3825	27.6369	0.008
biodiesel RP	0.08760	351.31	−0.8827	4.2086	0.005
biodiesel SP	0.08589	576.64	−2.3249	26.9757	0.007
biodiesel SRP	0.08280	496.92	−1.8604	19.8567	0.008
global AAD %[a]					0.007

[a] Global AAD % = $(\Sigma \mathrm{AAD}/N_s) \times 100$, where N_s is the number of systems studied.

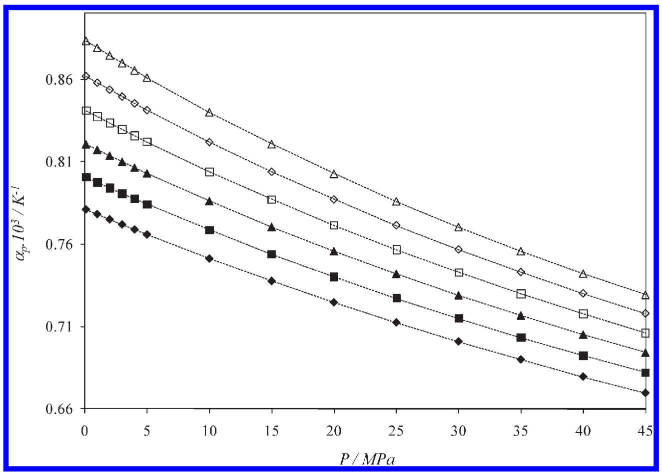

Figure 2. Isotherms for the isobaric expansion coefficient, α_P, of rapeseed biodiesel (◆, 283.15 K; ■, 293.15 K; ▲, 303.15 K; □, 313.15 K; ◇, 323.15 K; △, 333.15 K).

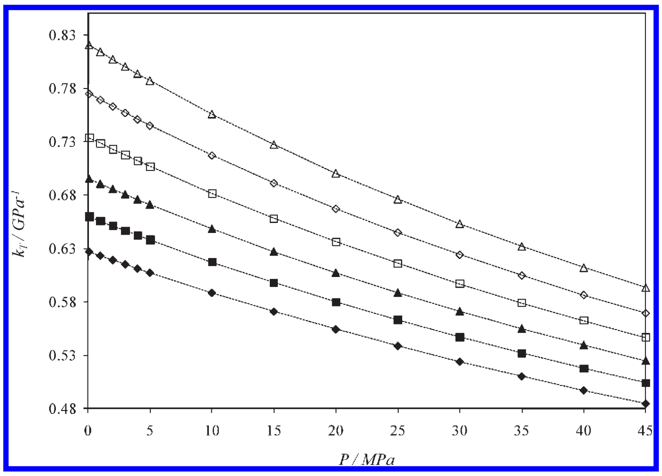

Figure 3. Isotherms for the isothermal compressibility coefficient, k_T, of rapeseed biodiesel (◆, 283.15 K; ■, 293.15 K; ▲, 303.15 K; □, 313.15 K; ◇, 323.15 K; △, 333.15 K).

presented in Table 6. They provide a good correlation for the experimental data for pure methyl esters and biodiesels, with a maximum deviation of 0.009% (Table 6). A graphical illustration is given in Figure 1 for the case of rapeseed biodiesel.

From the modified Tait−Tammann equation, it was also possible to compute isothermal compressibility coefficients, k_T, and isobaric expansion coefficients, α_P. These properties are partial derivatives of the specific volume as a function of the pressure or temperature, respectively. Examples of both properties in the temperature and pressure ranges studied are presented for rapeseed biodiesel in Figures 2 and 3, respectively. These property values for all of the pure compounds and mixtures considered here are also presented as Supporting Information.

By applying the propagation law of errors in eqs 5 and 7 and taking into account the uncertainties in the density, temperature, pressure, and coefficients involved in eqs 5 and 7, we obtained an uncertainty of the order of ±0.05 GPa^{-1} for k_T and $\pm 5 \times 10^{-4}$ K^{-1} for α_P.

For the compounds investigated here, FAMEs and biodiesels, isobaric expansion coefficient values decrease with an increasing ester chain length and pressure and, as previously observed,[14,16] increase with an increasing temperature. Expansion coefficient values are similar between them for the considered FAMEs and biodiesels and also similar to other values reported in the literature for fatty acid esters and biodiesels.[12−16] Colza biodiesel has the highest and the lowest α_P values, at the lowest pressure and highest temperature and at the highest pressure and lowest temperature, of 0.88 and 0.67, respectively. A larger isobaric expansion coefficient means a larger engine power loss because of fuel heating.

Isothermal compressibility coefficients, k_T, decrease when the pressure increases and when the temperature decreases. The selected FAMEs and biodiesels present similar values for the isothermal compressibility coefficients, values raging from 0.67 and 0.88 in the temperature and pressure ranges selected here. Again, similar values were also found in the literature for the compressibility coefficients of soybean[13] and rapeseed[12] biodiesels.

The experimental data reported here were also used to evaluate the predictive character of the CPA EoS in describing high-pressure density data. Fatty acid esters are non-self-associating compounds, and therefore, only the three CPA pure compound parameters of the physical term (a_0, c_1, and b) are required to describe these compounds. CPA EoS parameters for several ester families were proposed in a previous work,[20] where it was also shown that the a_0, c_1, and b parameters follow trends with the ester carbon number. Correlations to compute these parameters were proposed, enabling us to estimate them for new compounds when pure compound data are scarce, as happened for liquid densities of the higher carbon number fatty acid esters. Parameters calculated from the proposed correlations are presented, for all of the esters found in the biodiesels studied, as Table 7 in the Supporting Information.

Using our recently published density data for several fatty acid esters that can be found in biodiesels,[14,15] it was also possible in this work to estimate CPA pure compound parameters for all of the FAMEs found in the biodiesel samples, compounds ranging from 15 to 25 carbon atoms and with up to three unsaturated bonds (Table 4), by a simultaneous regression of pure component data. Critical temperatures (T_c) for these esters were determined from the group contribution method by Wilson

Table 7. FAME CPA Pure Compound Parameters and Modeling Results

				AAD %		
methyl ester	a_0 (J m^3 mol^{-2})	c_1	b ($\times 10^4$, m^3 mol^{-1})	P	ρ	T (K) range
C12	6.7139	1.5340	2.3010	0.83	0.60	283.15−353.15
C14:0	8.0272	1.6089	2.6361	0.45	0.52	298.15−353.15
C16	7.4198	2.2873	2.9749	1.46	0.62	308.15−363.15
C16:1	9.2554	1.7805	2.9564	2.38	1.21	287.15−363.15
C18	10.1303	1.9196	3.3111	0.39	0.68	313.1−363.15
C18:1	10.5075	1.8212	3.2485	0.81	0.74	283.15−353.15
C18:2	8.9943	2.1597	3.1714	1.37	0.66	278.15−363.15
C18:3	8.6712	2.1722	3.0949	1.18	1.03	278.15−373.15
C20	13.4696	1.6123	3.7121	0.78	0.85	323.15−373.15
C20:1	12.5293	1.7143	3.5792	5.98	1.22	278.15−373.15
C22	16.2713	1.4963	4.0503	0.34	0.71	333.15−373.15
C22:1	15.3112	1.5933	3.9168	4.73	1.86	278.15−363.15
C24	19.3150	1.4045	4.3953	0.13	0.65	338.15−373.15
global AAD %[a]				1.60	0.87	

[a] Global AAD % = $(\Sigma \mathrm{AAD}/N_s) \times 100$, where N_s is the number of systems studied.

Table 8. CPA EoS Modeling Results for High-Pressure Densities

	AAD %	
	ρ (0.1−45 MPa)[a]	ρ (0.1−45 MPa)[b]
methyl laurate	4.47	0.59
methyl myristate	5.86	0.99
methyl oleate	3.24	0.84
biodiesel S		0.79
biodiesel R		2.51
biodiesel P		1.13
biodiesel RP		1.07
biodiesel SR		0.82
biodiesel SP		1.25
biodiesel SRP		0.89
global AAD %		1.09

[a] With FAME CPA pure compound parameters from correlations. [b] With FAME CPA pure compound parameters correlated from pure component data.

and Jasperson[33] that was previously assessed to be the best method to compute this property for methyl esters,[34] and vapor pressures were taken from Chickos et al.,[35] Lipkind et al.,[36] and Yuan et al.[37] Parameter values are presented at Table 7, along with liquid density and vapor pressure deviations. An excellent description of vapor pressures and liquid densities for all of the FAMEs is achieved with the CPA EoS, with global average deviations of 1.6 and 0.9%, respectively.

With the CPA pure compound parameters for all of the pure FAMEs that compose the selected biodiesels, the CPA EoS was applied to predict the experimental high-pressure density data. First, both sets of parameters obtained from the correlations and pure compound data regression were used to predict the pure FAME high-pressure density data. Higher deviations are obtained when using pure compound parameters computed from correlations, as presented at Table 8, with deviations below 6%.

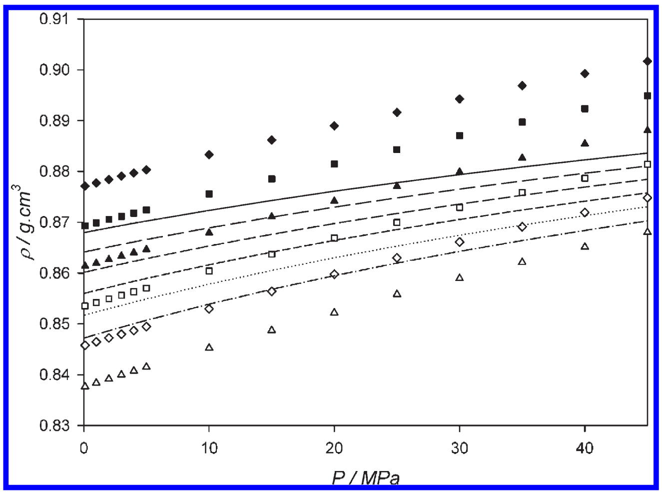

Figure 4. Density isotherms for methyl laurate. Experimental data (◆, 283.15 K; ■, 293.15 K; ▲, 303.15 K; □, 313.15 K; ◇, 323.15 K; △, 333.15 K) and CPA EoS results using pure compound parameters regressed from component data (solid line, 283.15 K; long dash line, 293.15 K; medium dash line, 303.15 K; short dash line, 313.15 K; dotted line, 323.15 K; dash−dot line, 333.15 K).

Results improved when using the regressed FAME CPA pure compound parameters, with the high-pressure experimental data for methyl laurate, methyl myristate, and methyl oleate being predicted with global average deviations inferior to 0.8%. Experimental and modeling results are depicted in Figure 4 for methyl laurate. The experimental data slope and range differ from the ones provided by the CPA EoS because of the characteristic inability of analytic EoSs to match the shape of the density temperature dependence. It is also worthy to note that higher deviations are obtained with the CPA EoS in comparison to the results obtained with the modified Tait−Tammann equation, as expected, because the EoS approach is applied in a totally predictive way and using a considerable inferior number of parameters.

The new CPA pure compound parameters for FAMEs proposed in this work were then applied to successfully predict

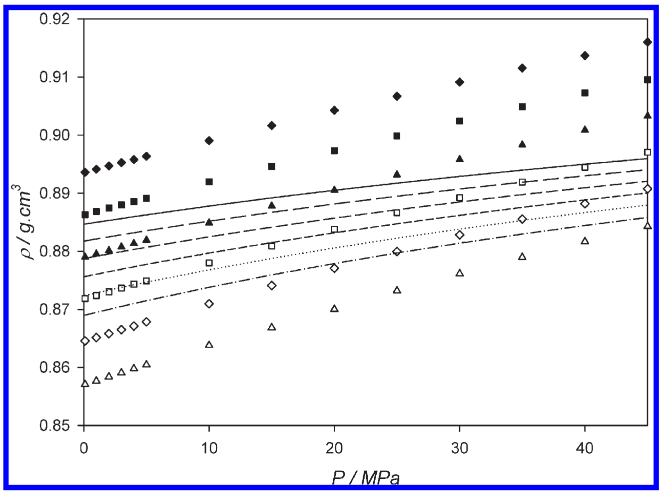

Figure 5. Density isotherms for soybean biodiesel. Experimental data (◆, 283.15 K; ■, 293.15 K; ▲, 303.15 K; □, 313.15 K; ◇, 323.15 K; △, 333.15 K) and CPA EoS results (solid line, 283.15 K; long dash line, 293.15 K; medium dash line, 303.15 K; short dash line, 313.15 K; dotted line, 323.15 K; dash−dot line, 333.15 K).

the experimental high-pressure density data for the methyl biodiesels from palm, soybean, and rapeseed oils and their binary and ternary mixtures. The CPA EoS is able to predict high-pressure density data for biodiesels with a maximum deviation of 2.5%. Results are depicted in Figure 5 for soybean biodiesel.

5. CONCLUSION

Europe aims to replace 20% of fossil fuels to alternative renewable fuels, such as biofuels, by 2020.[1] For the introduction of common rail engines in new vehicles, the description of high-pressure biodiesel densities is of primary importance to the fuel and automotive industries. New experimental high-pressure density measurements were performed for three FAMEs and seven biodiesels, overcoming the lack of available experimental data.

The experimental data were correlated with the modified Tait−Tammann equation and predicted by the CPA EoS. New CPA EoS parameters were computed in this work for the 13 different fatty acid esters that constitute the biodiesel samples selected for this work, from C_{15} to C_{25} and with up to three unsaturated bonds.

The CPA EoS can predict the high-pressure density data of pure FAMEs and biodiesels with a maximum deviation of 2.5%, showing to be an adequate model to predict properties of relevance for biodiesel fuels.

■ ASSOCIATED CONTENT

Ⓢ Supporting Information. Values for the isothermal compressibility coefficients, k_T, and isobaric expansion coefficients, α_P, in the selected temperature and pressure ranges for all of the pure compounds and mixtures studied and CPA pure compound parameters for esters obtained from ester carbon number correlations. This material is available free of charge via the Internet at http://pubs.acs.org.

■ AUTHOR INFORMATION

Corresponding Author

*Telephone: +351-234401507. Fax: +351-234370084. E-mail: mbelo@ua.pt (M.B.O.); jcoutinho@ua.pt (J.A.P.C.).

■ ACKNOWLEDGMENT

Maria Jorge Pratas acknowledges the financial support from Fundação para a Ciência e a Tecnologia through the Ph.D. Grant SFRH/BD/28258/2006.

■ NOMENCLATURE

Abbreviations

AAD = average absolute deviation, $(\sum_{i=1}^{N_p}|(\text{exptl}_i - \text{calcd}_i)/\text{exptl}_i|)/N_p$
CPA = cubic-plus-association
EoS = equation of state
FAME = fatty acid methyl ester
LLE = liquid−liquid equilibria
S = soybean
R = rapeseed
P = palm
SR = soybean + rapeseed
RP = rapeseed + palm
SP = soybean + palm
SRP = soybean + rapeseed + palm
VLE = vapor−liquid equilibria

List of Symbols

a = energy parameter in the physical term of the CPA EoS (J m^3 mol^{-2})
a_0 = parameter for calculating a (J m^3 mol^{-2})
a_1 = eq 2 coefficient (kg m^{-3})
a_2 and a_3 = eq 2 coefficients (kg m^{-3} K^{-1} and kg m^{-3} K^{-2}, respectively)
b = co-volume parameter in the physical term of the CPA EoS (m^3 mol^{-1})
b_1 and C = eq 3 coefficients (b_1 in MPa)
b_2 = eq 3 coefficient (MPa K^{-1})
b_3 = eq 3 coefficient (MPa K^{-2})
k_{ij} = binary interaction parameter
k_T = isothermal compressibility coefficient (GPa^{-1})
P = vapor pressure (Pa)
R = gas constant (J mol^{-1} K^{-1})
T = temperature (K)
V_m = molar volume (m^3 mol^{-1})
x = mole fraction
w = mass fraction
Z = compressibility factor

Greek Letters

α_P = isobaric expansion coefficient (K^{-1})
ρ = density (kg m^{-3})

Subscripts

c = critical
calcd = calculated
exptl = experimental
i and j = pure component indexes
r = reduced

Superscripts

assoc. = association
phys. = physical

■ REFERENCES

(1) Malca, J.; Freire, F. *Renewable Sustainable Energy Rev.* **2011**, *15*, 338–351.

(2) Demirbas, A. *Appl. Energy* **2009**, *86*, S108–S117.

(3) Ma, F. R.; Hanna, M. A. *Bioresour. Technol.* **1999**, *70*, 1–15.

(4) Van Gerpen, J. *Fuel Process. Technol.* **2005**, *86*, 1097–1107.

(5) Demirbas, A. *Energy Policy* **2007**, *35*, 4661–4670.

(6) Lee, S. W.; Tanaka, D.; Kusaka, J.; Daisho, Y. *JSAE Rev.* **2002**, *23*, 407–414.

(7) Dzida, M.; Prusakiewiez, P. *Fuel* **2008**, *87*, 1941–1948.

(8) Boudy, F.; Seers, P. *Energy Convers. Manage.* **2009**, *50*, 2905–2912.

(9) Bora, D. K. *J. Sci. Ind. Res.* **2009**, *68*, 960–963.

(10) Boehman, A. L.; Morris, D.; Szybist, J.; Esen, E. *Energy Fuels* **2004**, *18*, 1877–1882.

(11) European Committee for Standardization (CEN). *European Standard EN 14214. Automotive Fuels—Fatty Acid Methyl Esters (FAME) for Diesel Engine—Requirements and Test Methods*; CEN: Brussels, Belgium, 2010; http://www.din.de.

(12) Aparicio, C.; Guignon, B.; Rodriguez-Anton, L. M.; Sanz, P. D. *J. Therm. Anal. Calorim.* **2007**, *89*, 13–19.

(13) Aparicio, C.; Guignon, B.; Rodríguez-Antón, L. M.; Sanz, P. D. *J. Agric. Food Chem.* **2007**, *55*, 7394–7398.

(14) Pratas, M. J.; Freitas, S.; Oliveira, M. B.; Monteiro, S. C.; Lima, A. S.; Coutinho, J. A. P. *J. Chem. Eng. Data* **2010**, *55*, 3983–3990.

(15) Pratas, M. J.; Freitas, S.; Oliveira, M. B.; Monteiro, S. C.; Lima, A. S.; Coutinho, J. A. P. *Ind. Eng. Chem. Res.* **2011**, *56*, 2175–2180.

(16) Pratas, M. J.; Freitas, S. V. D.; Oliveira, M. B.; Monteiro, S. C.; Lima, A. S.; Coutinho, J. A. P. *Energy Fuels* **2011**, *25*, 2333–2340.

(17) Dymond, J. H.; Malhotra, R. *Int. J. Thermophys.* **1988**, *9*, 941–951.

(18) Oliveira, M. B.; Ribeiro, V.; Queimada, A. J.; Coutinho, J. A. P. *Ind. Eng. Chem. Res.* **2011**, *50*, 2348–2358.

(19) Oliveira, M. B.; Queimada, A. J.; Coutinho, J. A. P. *Ind. Eng. Chem. Res.* **2010**, *49*, 1419–1427.

(20) Oliveira, M. B.; Varanda, F. R.; Marrucho, I. M.; Queimada, A. J.; Coutinho, J. A. P. *Ind. Eng. Chem. Res.* **2008**, *47*, 4278–4285.

(21) Pineiro, M. M.; Bessieres, D.; Gacio, J. M.; Saint-Guirons, H.; Legido, J. L. *Fluid Phase Equilib.* **2004**, *220*, 127–136.

(22) Pineiro, M. M.; Bessieres, D.; Legido, J. L.; Saint-Guirons, H. *Int. J. Thermophys.* **2003**, *24*, 1265–1276.

(23) Kontogeorgis, G. M.; Michelsen, M. L.; Folas, G. K.; Derawi, S.; von Solms, N.; Stenby, E. H. *Ind. Eng. Chem. Res.* **2006**, *45*, 4855–4868.

(24) Kontogeorgis, G. M.; Michelsen, M. L.; Folas, G. K.; Derawi, S.; von Solms, N.; Stenby, E. H. *Ind. Eng. Chem. Res.* **2006**, *45*, 4869–4878.

(25) Oliveira, M. B.; Coutinho, J. A. P.; Queimada, A. J. *Fluid Phase Equilib.* **2007**, *258*, 58–66.

(26) Michelsen, M. L.; Hendriks, E. M. *Fluid Phase Equilib.* **2001**, *180*, 165–174.

(27) Wu, J. Z.; Prausnitz, J. M. *Ind. Eng. Chem. Res.* **1998**, *37*, 1634–1643.

(28) Muller, E. A.; Gubbins, K. E. *Ind. Eng. Chem. Res.* **2001**, *40*, 2193–2211.

(29) Oliveira, M. B.; Miguel, S. I.; Queimada, A. J.; Coutinho, J. A. P. *Ind. Eng. Chem. Res.* **2010**, *49*, 3452–3458.

(30) Oliveira, M. B.; Queimada, A. J.; Coutinho, J. A. P. *J. Supercrit. Fluids* **2010**, *52*, 241–248.

(31) Follegatti-Romero, L. A.; Lanza, M.; Batista, F. R. M.; Batista, E. A. C.; Oliveira, M. B.; Coutinho, J. A. P.; Meirelles, A. J. A. *Ind. Eng. Chem. Res.* **2010**, *49*, 12613–12619.

(32) Rodrigues, J.; Cardoso, F.; Lachter, E.; Estevão, L.; Lima, E.; Nascimento, R. *J. Am. Oil Chem. Soc.* **2006**, *83*, 353–357.

(33) Poling, B.; Prausnitz, J.; O'Connell, J. *The Properties of Gases and Liquids*; McGraw-Hill: New York, 2001.

(34) Lopes, J. C. A.; Boros, L.; Krahenbuhl, M. A.; Meirelles, A. J. A.; Daridon, J. L.; Pauly, J.; Marrucho, I. M.; Coutinho, J. A. P. *Energy Fuels* **2008**, *22*, 747–752.

(35) Chickos, J. S.; Zhao, H.; Nichols, G. *Thermochim. Acta* **2004**, *424*, 111–121.

(36) Lipkind, D.; Kapustin, Y.; Umnahanant, P.; Chickos, J. S. *Thermochim. Acta* **2007**, *456*, 94–101.

(37) Yuan, W.; Hansen, A. C.; Zhang, Q. *Fuel* **2005**, *84*, 943–950.

Experimental Density Data for the Rapessed Biodiesel

	$(\rho \pm 0.1)/(\mathrm{kg\cdot m^{-3}})$ at $(T\pm 5\mathrm{x}10^{-2})/\mathrm{K}$					
$(p\pm 2\mathrm{x}10^{-3})/\mathrm{MPa}$	**283.2**	**293.2**	**303.2**	**313.2**	**323.2**	**333.2**
0.10	891.4	884.4	877.4	869.9	862.7	855.2
1.00	891.9	885.0	877.9	870.5	863.2	855.8
2.00	892.5	885.6	878.5	871.1	863.9	856.5
3.00	893.1	886.1	879.1	871.7	864.5	857.2
4.00	893.6	886.7	879.7	872.4	865.2	857.9
5.00	894.2	887.3	880.3	873.0	865.9	858.5
10.00	896.6	890.0	883.2	876.0	869.1	861.9
15.00	899.5	892.8	886.1	879.0	872.2	865.0
20.00	902.1	895.5	888.9	881.9	875.1	868.1
25.00	904.6	898.1	891.5	884.7	878.0	871.3
30.00	907.0	900.5	894.1	887.4	881.0	874.2
35.00	909.3	903.0	896.6	890.0	883.6	877.0
40.00	911.6	905.4	899.2	892.5	886.2	879.7
45.00	913.8	907.7	901.6	895.0	888.8	882.5